

# Structural Properties of Massive Young Clusters

Jesús Maíz-Apellániz

*Space Telescope Science Institute<sup>1</sup>, 3700 San Martin Drive, Baltimore, MD 21218, U.S.A.*

## ABSTRACT

We have retrieved multicolor WFPC2/HST data from the STScI archive for 27 nearby Massive ( $\gtrsim 3 \cdot 10^4 M_{\odot}$ ) Young ( $< 20$  Myr) star Clusters (MYCs). The data represents the most-complete-to-date sample of clearly resolved MYCs. We have analyzed their structural properties and have found that they can be classified as either Super Star Clusters (SSCs) or as Scaled OB Associations (SOBAs). SSCs have a compact core possibly surrounded by a halo while SOBAs have no core. A morphological sequence can be established from SSCs with weak halos to SSCs with strong halos to SOBAs and we propose that this is linked to the original mass distribution of the parent giant molecular clouds. Our results indicate that a significant fraction of the stars in MYCs dissipate on timescales of 10 Gyr or less due to the extended character of some of the clusters. Also, SSCs with ages  $< 7$  Myr have smaller cores on average than those with ages  $> 7$  Myr, confirming predictions of numerical simulations with mass loss.

*Subject headings:* galaxies: star clusters — galaxies: starburst — techniques: high angular resolution

## 1. INTRODUCTION

Traditionally, star clusters have been classified as globular or open clusters. Globular clusters are old ( $\sim 10$  Gyr), massive ( $3 \cdot 10^4 - 3 \cdot 10^6 M_{\odot}$ ), metal-poor, and spherically-symmetric members of a halo population while open clusters are young ( $\lesssim 1$  Gyr), low-mass ( $< 5 \cdot 10^3 M_{\odot}$ ), metal-rich, and asymmetric members of a galactic disk. This classification

---

<sup>1</sup>The Space Telescope Science Institute is operated by the Association of Universities for Research in Astronomy, Inc. under NASA contract No. NAS5-26555.

is based on the cluster population of the Milky Way, where the dichotomy between the two types of clusters was first observed, but the situation is not the same for all galaxies. A clear example of this is the LMC, where we have 13 – 15 classical ( $\approx 13$  Gyr old) globular clusters (GCs) but also several intermediate age (1 – 3 Gyr old) and many young clusters (Da Costa 2001). Some of the young and intermediate LMC clusters have masses in the range  $10^4 - 10^5 M_\odot$ , similar to or slightly smaller than those of Galactic GCs and are usually called in the literature “rich clusters” (see, e.g., Elson & Fall 1985). Most of those rich clusters are part of the galactic disk (Freeman et al. 1983), so it is obvious that the traditional Galactic classification cannot be directly extended to the LMC. Furthermore, in recent years it has been established that the Milky Way also has its own LMC-like rich clusters (Moffat et al. 1994; Figer et al. 1999; Knödlseeder 2000), so the traditional classification cannot be strictly applied even to the Galaxy.

Other clusters which do not fit into the traditional classification are Super Star Clusters (or SSCs), first described in the nearby galaxies NGC 1569 and NGC 1705 by Arp & Sandage (1985) and Melnick et al. (1985). SSCs are compact Massive ( $\gtrsim 3 \cdot 10^4 M_\odot$ ) Young Clusters<sup>2</sup> (or MYCs) which, at first, could not be resolved from the ground and were mistaken for foreground stars. HST imaging (O’Connell et al. 1994) was needed to establish their nature and to determine that they indeed belonged to their apparent host galaxies. Another interesting object is R136, the core of 30 Doradus in the LMC, which was once suspected to be a supermassive  $1\,000 - 3\,000 M_\odot$  star until Weigert & Baier (1985) used holographic speckle interferometry to resolve it. Now it is clear that it is just another example of a compact MYC.

The main reason why the traditional (Galactic-biased) classification does not include rich clusters or MYCs is that the Milky Way is not currently in an active intense-star-formation phase, which accounts for the scarcity of those objects in the Galaxy. Furthermore, extinction at low latitudes severely hampers the detection of distant Galactic clusters. At the opposite side of the activity spectrum from the Milky Way we have starburst and interacting galaxies such as the “Antennae” (NGC 4038/4039), where we observe many clusters with masses larger than  $10^4 M_\odot$  and ages less than 1 Gyr (Zhang & Fall 1999). In between, we have dwarf starburst galaxies like NGC 4214 or NGC 5253, where several massive clusters with ages of less than 100 Myr are visible in the central regions.

Another problem with cluster classification is the distinction between bound (or real)

---

<sup>2</sup>Note that, as is usually the case when classifying astronomical objects, no uniform definition of how massive a cluster has to be to be included in the “massive” category appears in the literature. Our choice is explained below.

clusters and associations, which are unbound groups that are slowly dispersed by the galactic tidal field. Both types of objects are formed from molecular clouds, with some of them being born as weakly bound clusters and later becoming associations due to mass loss and tides, thus complicating the distinction<sup>3</sup>. It is only with the use of detailed kinematic data that it is possible to differentiate between bound clusters and associations, but such information is usually lacking for young extragalactic objects. Therefore, in this paper we will use the term cluster in its broad sense of a stellar group formed from a single cloud, and we will not assume that it is a bound object.

What is the connection between massive young clusters and globular clusters? Do all MYCs evolve to become GCs or do only a fraction survive after 10 Gyr? The keys to answer that question are the mass and the structure of the cluster: only massive ( $\gtrsim 3 \cdot 10^4 M_{\odot}$ ) clusters of the right size (half-light radius  $\approx 1 - 10$  pc) have a good chance of survival in a Hubble time scale (Fall & Rees 1977). Therefore, we need to determine the distribution of masses and radii of MYCs in order to establish how many of them will become the GCs of the future. As it happens most of the times in astronomy, it is easier to measure the total light output of an object than its mass, so most cluster mass estimates are based on an assumed IMF or  $M/L$  ratio. Thus, only a few SSC masses have been directly measured (Ho & Filippenko 1996, 2001; Gallagher & Smith 1999; Larsen 2001), with the results (in the approximate range  $10^5 - 10^6 M_{\odot}$ ) being consistent with the minimum required mass for survival.

In this paper we will concentrate on the second key by carrying an analysis of the radial structure of MYCs in order to answer the questions: Do all clusters have similar sizes? Do they all have similar core/halo mass ratios? How many clusters are likely to be bound? Previous studies have run into a problem: most galaxies with large numbers of MYCs are too far away to easily resolve the clusters, even with HST (e.g., the Antennae), so they had to deal with a large fraction of only-partially resolved objects. In other cases (e.g., M82), distance is not a problem but extinction is, since large-scale starbursts tend to be shrouded in dust. There is actually not a single example of a galaxy with a large sample of MYCs which is not affected by heavy extinction and which is located at a distance where present instrumentation can easily resolve the clusters. Therefore, if we want to build a well-resolved sample large enough to be useful to study the structural properties of MYCs we will need to compile our list from objects in several nearby galaxies.

---

<sup>3</sup>We are referring here to processes that take place in Myr to Gyr time scales. In the long term all clusters are expected to dissolve, maybe leaving a central black hole, but for massive clusters the time scales involved can be much longer than  $10^{10}$  years and they can therefore be considered as bound in a first-order approximation.

In section 2 we present our data describing the sample, showing our measured values, and commenting on individual clusters. In section 3 we discuss our results and in section 4 we present a summary.

## 2. DATA

### 2.1. The sample

We have searched the HST archive for WFPC2 images of resolved MYCs in nearby galaxies and selected the objects which matched the following criteria:

1. In order to be able to measure the structural properties of the objects in our sample without introducing any significant bias, we selected only clusters within a radius of 5 Mpc (but see below for I Zw 18). This criterion eliminates, for example, the SSCs in He 2-10 (Johnson et al. 2000) and the “Antennae” clusters (Whitmore et al. 1999).
2. We selected MYCs with  $M_{V,\max}$  (the age-corrected  $M_V$ , see below)  $< -11$ , which eliminates some clusters like NGC 2363-B (Drissen et al. 2000). This criterion minimizes the confusion regarding the extension of the cluster (dimmer objects are harder to distinguish from the background and nearby clusters) and selects only the most massive clusters. Indeed, a  $3 \cdot 10^4 M_\odot$  cluster is expected from evolutionary synthesis models (Cerviño et al. 2001; Leitherer et al. 1999) to have an  $M_{V,\max}$  between  $-11$  and  $-12$  (the exact value depends on the metallicity and the IMF at low masses), a prediction confirmed by the measured masses (Ho & Filippenko 2001). Thus, by using this criterion we are sampling the likely predecessors of the GCs of the future.
3. Only clusters with ages less than 20 Myr were included. This criterion eliminates clusters like NGC 4214-III (Maíz-Apellániz et al. 2001) and NGC 5253-II and -III (Calzetti et al. 1997). Older clusters tend to have more imprecise ages and values of  $M_{V,\max}$ .
4. Dust-enshrouded clusters were also discarded due to the strong geometrical distortions induced by differential extinction around them. In this category there are highly-obscured objects like some of the ones in M82 (Gallagher & Smith 1999) and clusters with compact or “filled” nebular emission (Maíz-Apellániz & Walborn 2001) like NGC 4214-II-A and II-B (Mackenty et al. 2000), NGC 5253-V (Calzetti et al. 1997), and NGC 2363-A (Drissen et al. 2000). Those objects have moderate-to high extinctions as well as strong nebular line emission and continuum with a compact spatial distribution which

resembles that of the stellar continuum, thus severely hampering their distinction. The objects selected for our sample have low extinctions ( $E(B - V) < 0.5$ ) with the only exception of the NGC 1569 clusters (where most of the extinction is of Galactic origin and rather uniform nature).

Twenty-seven clusters in eight galaxies were included in our sample. They are listed in Table 1, along with the HST proposal IDs for the data. The clusters selected are very bright and in most cases they are among the most conspicuous optical structures in their host galaxies. We believe our data to be an over 50% complete sample of low-extinction massive ( $M_{V,\text{max}} < -11$ ) young (age  $< 20$  Myr) clusters within 5 Mpc. The largest degree of uncertainty is caused by the poorly known distances: some galaxies like NGC 1705 may actually be farther away than 5 Mpc while other ones which harbor good candidates (e.g. NGC 6946) may actually be closer.

Given that most galaxies were observed under diverse proposals, the number and selection of filters available is very different for each of the clusters. In order to make the data more uniform, two optical bands were selected in each case:  $U$  (F336W or F380W, but see below for the NGC 2403 case) and  $V$  (F555W or F547M, see below for the NGC 1705 case). The  $U$  data will be our main source to study the structure of the clusters. We chose that band because it is the best optical tracer for the young stellar continuum, is little affected by nebular contamination, has archival data available for all but one of our galaxies, and has the narrowest PSF. The differences between the two filters are small enough that no significant variations in the spatial structure should appear. The  $U$  images are displayed in Figs. 1, 2, and 3. The  $V$  data will be used to obtain absolute magnitudes. In this sense it is preferred to the  $U$  data because of its lower sensitivity to extinction. F555W is very similar to the Johnson  $V$  filter (for the age range of interest, the  $(F555W - V)$  colors are  $\approx 0.02$ , Holtzman et al. 1995). F547M is narrower than F555W but is centered at a very similar wavelength, so the measured colors should be almost identical in most cases. It is actually preferred to F555W due to its much lower sensitivity to nebular contamination. When strong nebular contamination was suspected in an F555W exposure, F502N ([O III]  $\lambda 5007$ ) and/or F656N ( $H\alpha$ ) WFPC2 images were used to eliminate this effect.

We compiled from the literature the available information regarding galaxy distances and cluster extinctions and ages (see Table 2). Five different methods are used in the available references to establish ages: color-magnitude diagrams, UV spectroscopy, optical spectral features (WR bands, Ca triplet), nebular equivalent widths, and integrated colors. Additionally, we used the data presented by Maíz-Apellániz & Walborn (2001) to detect the existence of  $H\alpha$  shells around the clusters and measure their sizes, thus placing an additional constraint on their ages:  $\sim 2$  Myr old clusters have small ( $\sim 10$  pc) shells around them,

$\sim 4$  Myr old clusters have larger ( $\sim 100$  pc) and usually broken shells, and for older clusters only diffuse  $H\alpha$  emission can be detected. Finally, we also measured the integrated colors in our data and used the Cerviño et al. (2001) models<sup>4</sup> to produce a self-consistent age and extinction (Maíz-Apellániz & Cerviño 2001). The final values for the ages and extinctions have quite different uncertainties depending on the number and quality of the sources. The distances to the Local Group clusters are quite precise (5 – 10% uncertainties) while the rest are not so well known ( $\sim 25\%$  uncertainties).

## 2.2. Results

For each of the clusters, we measured the integrated  $m_V$ . We used the Cerviño et al. (2001) models to correct for age differences by calculating the dimming between an age of 4 Myr (the approximate age at which a cluster attains its maximum optical brightness) and the current age. We then introduced the values of the distance and extinction to calculate  $M_{V,\max}$ , the  $M_V$  of the cluster at an age of 4 Myr. The values are listed in Table 3. No attempt has been made to estimate individual errors for  $M_{V,\max}$ , but for clusters outside the Local Group the typical uncertainties are of the order of 1 magnitude, with the dominant source being the uncertainty in the distance and, to a lesser degree, the age. The measurement uncertainties in  $m_V$  itself are only relevant for Local Group objects, where the total errors can be estimated as being less than 0.5 magnitudes.

Analyzing the  $U$  band images we discovered that some clusters have a distinct compact core (Figs. 1 and 2) while in others no core is readily apparent (Fig. 3). Compact cores are easily distinguished because they have integrated values of  $M_{V,\max} < -10$  within a radius of  $\lesssim 3$  pc (see Table 3), which is  $\gtrsim 2$  magnitudes brighter than the most luminous surrounding stars. Most cores show an approximate circular symmetry but some are double or elongated. Massive clusters with no core have the appearance of an OB association in terms of shape and size but they are much more massive than the known Galactic ones. We propose here the use of the term “Scaled OB Association” (or SOBA) to refer to them, following a previous suggestion by Hunter (1999). SOBAs are quite asymmetric extended objects with no well-defined center<sup>5</sup> and are likely to be weakly bound, if bound at all.

---

<sup>4</sup>Available from <http://www.laeff.esa.es/~mcs/model>.

<sup>5</sup>This lack of a well defined center makes the values of  $M_{V,\max}$  within 3 pc listed in Table 3 for SOBAs somewhat arbitrary, with a different choice of aperture probably producing results different by up to 0.5 magnitudes. Note, however, that with the only exception of the I Zw 18 clusters we always tried to center our apertures at the brightest point source, so other choices would only probably make  $M_{V,\max}$  within 3 pc

One difference is also readily apparent between the clusters with a compact core (or compact clusters, for short) in Fig. 1 and those in Fig. 2: The first ones do not have a halo or only a weak one around the core while for the second ones the halo is as luminous or even more so than the core itself. We will refer to the clusters in Fig. 1 as compact clusters with weak halos and to those in Fig. 2 as compact clusters with strong halos. Halos have a structure similar to that of SOBAs (Fig. 4) and their approximate center usually does not coincide with the cluster core.

We would like to test whether this morphological classification corresponds to real structural differences or not. In particular, we would like to know whether the core-halo structure of the objects in Fig. 2 is caused by the existence of two distinct structural components or whether the core is just the central region of an extended one-component structure. A way to test this would be to try to fit a King profile (King 1962) in each case. Unfortunately, this is not possible due to the diverse spatial resolution of the data: even though all cores are resolved in the sense of being at least significantly broader than nearby stars, they are not always resolved to the point of being able to unambiguously measure the profile parameters. However, we can settle for a poor-man’s version of this procedure by measuring the  $U$ -band  $r_{1/4}$ ,  $r_{1/2}$ , and  $r_{3/4}$ , the one-quarter, one-half, and three-quarters light-radii<sup>6</sup>, and constructing the ratio  $\alpha = r_{1/2}^2/(r_{1/4}r_{3/4})$ . Single-component King profiles with reasonable values of  $r_t/r_c$  (the ratio of the tidal to the core radii) are expected to have values of  $\alpha$  very close to 1.0, as shown in Fig. 5. On the other hand, clusters with two components with  $\lesssim 50\%$  of the light originating in the compact one and  $\gtrsim 50\%$  in the extended one should have values of  $r_{1/4}$  (determined fundamentally by the compact component) smaller than expected for given ones of  $r_{1/2}$  and  $r_{3/4}$  (determined fundamentally by the extended component), which should lead to values of  $\alpha$  larger than one. A problem associated with these measurements (or with any other measurement of cluster brightness profiles) is the definition of the total light radius, which is needed for a correct subtraction of the background. This was done by selecting an initial guess from a visual inspection of the image and then modifying it until the area just outside the total light radius had an approximately flat intensity and color radial profile. The adjacent area was then used to determine the background. When two clusters were close to each other, masks were used to avoid mutual contamination.

In Table 3 we show the measured values for  $r_{1/4}$ ,  $r_{1/2}$ , and  $r_{3/4}$ . The  $r_{1/4}$  values have been corrected for the finite value of the PSF width but the corrections turned out to be

---

dimmer.

<sup>6</sup>Note that in a preliminary version of this work (Maíz-Apellániz & Walborn 2001),  $r_{1/2}$  was defined as applying only to the cluster core in the case of a compact cluster. Here,  $r_{1/4}$ ,  $r_{1/2}$ , and  $r_{3/4}$  refer to the whole cluster always.

unimportant in most cases. The values of  $\alpha$  as a function of  $r_{1/2}$  are plotted in Fig. 5. There we can see that compact clusters with weak halos (with one exception, NGC 1569-C, one of the clusters with a double core) and SOBAs are reasonably well adjusted to the prediction of a single component King model ( $\alpha \approx 1$ ). However, compact clusters with strong halos all have values of  $\alpha$  clearly greater than 1, indicating that they are indeed made out of two different structural components. Furthermore, the fact that the three cluster classes occupy different areas of this  $r_{1/2} - \alpha$  diagram reinforces the reality of the differences suggested by the morphological classification.

We can then conclude that the MYCs in our sample are made out of two structural components: compact cores with half-light radii of  $< 5$  pc and extended halos with half-light radii  $> 15$  pc. In some cases one of the two components is absent or weak, and then we have a compact cluster with a weak halo or a SOBA. In other occasions both have a significant contribution and the result is a compact cluster with a strong halo. However, no single-component clusters with half-light radii of  $\sim 10$  pc are detected in our sample, as evidenced by the “hole” around  $r_{1/2} \approx 10$  pc,  $\alpha \approx 1$  in Fig. 5.

Other studies (Meurer et al. 1995; Whitmore et al. 1999) have not detected the compact cluster-SOBA dichotomy. Besides the problem with spatial resolution at large distances and the mixture of high-mass and low-mass clusters, there is another explanation for this lack of detection. As shown in Fig. 6, when  $r_{1/2}$  is used as a measurement of cluster size, compact clusters with strong halos appear as intermediate size objects which fill the gap between the other two classes, so the size histogram does not show a strong bimodality. However, when  $r_{1/4}$  is used, the two peaks are quite clear. This is explained by the fact that for compact clusters  $r_{1/4}$  is determined fundamentally by the core and is more or less independent of the strength of the halo (though it may depend on whether the core itself is double or elongated).

### 2.3. Object nomenclature and notes

**30 Doradus, NGC 595, and NGC 604:** These clusters are the three brightest low-extinction MYCs in the Local Group. 30 Doradus is in the LMC and NGC 595 and NGC 604 are in M33. The core of 30 Doradus, R136, fits easily in the PC field of view (Hunter et al. 1995) but the halo is much more extended and we had to use the 5 WFPC2-fields mosaic generated by Walborn et al. (2001) in order to cover it. R136 is the archetype of compact clusters with a strong halo, since  $\approx 90\%$  of its total integrated light originates there. The images of 30 Doradus and NGC 595 shown in Figs. 2 and 3, respectively, were convolved with a gaussian kernel for display purposes.



**I Zw 18-I and -II:** These low-metallicity clusters are included even though I Zw 18 is at a distance of 10 Mpc because their extended character makes them easy to resolve. They are sometimes called I Zw 18-NW and -SE, respectively.

**NGC 1569 clusters:** NGC 1569-A has a double core, with the two components separated by only 2 pc in the plane of the sky and with an  $\approx 1.3$  magnitude difference between them (De Marchi et al. 1997). The detection of both WR emission features and the near-IR Ca II triplet in absorption in their unresolved spectrum led González Delgado et al. (1997) to suggest an age difference of  $\approx 6$  Myr between the two. However, the measured color difference between the two cores is small (with some likely mutual contamination), so it is not straightforward to test this hypothesis with the available data (De Marchi et al. 1997) and here we will treat NGC 1569-A as a single cluster. NGC 1569-A is the archetype of compact clusters with a weak halo, since only  $\lesssim 5\%$  of its total integrated light originates there. NGC 1569-C was classified as number 10 by Hunter et al. (2000). As pointed out by Buckalew et al. (2000), two cores can be identified (separation  $\approx 4$  pc). Note the existence of a significant internal extinction compared to NGC 1569-A and -B. The anomalous location of NGC 1569-C in Fig. 6 (it is the only compact cluster with a weak halo with  $\alpha$  significantly greater than 1) is caused by the double nature of its core.

**NGC 1705-I-A and -I-B:** NGC 1705-I-A is the bright SSC described by Melnick et al. (1985). NGC 1705-I-B is the second brightest cluster in the galaxy and is located at a projected distance of  $1''.0$  (24 pc) from NGC 1705-I-A, which we consider large enough to treat them as individual clusters. In O’Connell et al. (1994) NGC 1705-I-B is referred to as cluster 35 and in Meurer et al. (1995) as NGC 1705-2. In most of the WFPC2 images of this galaxy available in the HST archive at the present time, NGC 1705-I-A is saturated, and in the ones in which it is not saturated, a tracking problem produced an elongated PSF, making them useless for our purposes of measuring the radial intensity profile. Fortunately, the saturation in the two F380W images with correct tracking is weak, affecting only the central  $3 \times 3$  pixels. Thus, we used the integrated photometry from the unsaturated F380W image with incorrect tracking to correct the flux in those central 9 pixels (only a 26% increase in the total number of counts was required). The measured value of  $r_{1/4}$  (corrected for saturation but not for the width of the PSF) is  $1.44 \pm 0.10$  pixels (compared to an  $r_{1/4}$  value for a point source of  $\approx 0.4$  pixels), with the exact value depending on how the extra flux is allocated inside the central 9 pixels. We can then conclude that the uncertainty introduced by the saturation correction in the value of  $r_{1/4}$  for NGC 1705-I-A is tolerable (i.e. it is much smaller than the one introduced by the uncertainty in the distance). Another problem we had to face was that in all of the F555W images available in the HST archive NGC 1705-I-A and -I-B are saturated, so  $m_V$  had to be obtained from O’Connell et al. (1994) and Ho & Filippenko (1996). Their values are consistent with our measured  $m_{F380W}$  and  $m_{F439W}$  and the known

colors of NGC 1705-I-A.

**NGC 2403 clusters:** We follow the nomenclature of Drissen et al. (1999). NGC 2403-I-A shows a weak core but we classified it as a SOBA because the value of  $M_{V,\max}$  within 3 pc is dimmer than  $-10$ . NGC 2403-IV is a compact cluster with a double core (separation  $\approx 7$  pc), as shown in Fig. 2. NGC 2403 is the only galaxy with no  $U$  observations available, so the filter with the most similar characteristics, F439W (WFPC2  $B$ ), was selected to analyze the structure of its clusters.

**NGC 4214 clusters:** We follow the nomenclature of Mackenty et al. (2000). NGC 4214-II-A and -B are not included in the sample because of strong nebular contamination. NGC 4214-III and -IV are excluded because they are older than 20 Myr. We adopt a distance of 4.1 Mpc but it should be noted that a preliminary analysis of WFPC2 stellar photometry (final results will be published as Maíz-Apellániz et al. 2001) indicates that the distance could be up to a factor of  $\sim 2$  smaller. Such a change would not alter our conclusions since its effects would be only to exclude NGC 4214-II-C and NGC 4214-VI from our sample (due to the  $M_{V,\max} < -11$  requirement) and maybe to change the classification of NGC 4214-I-C.

**NGC 4449-N-1 and -N-2:** These two objects are located in the nuclear region (hence the designation N) and they are the two brightest clusters in the galaxy. In Gelatt et al. (2001) they are called 1 and 31, respectively. Both cluster cores are separated by  $\approx 22$  pc (enough to consider them as individual clusters) and have elongated shapes. They appear to be in the process of being torn apart by tidal forces.

**NGC 5253 clusters:** We follow the nomenclature of Calzetti et al. (1997) but using roman numerals instead of arabic ones for consistency with the rest of our numbered clusters. NGC 5253-V is not included in our sample due to its heavy extinction. NGC 5253-II and -III are also excluded because they are older than 20 Myr. NGC 5253-IV has a double core (separation  $\approx 4.5$  pc).

### 3. DISCUSSION

#### 3.1. Consequences of the morphological dichotomy

The different sizes of the cores and halos (including SOBAs in this last category) of MYCs and their similar masses imply that the orbital time scales must be very different. Thus, a star in a typical core has an orbital period of  $0.3 - 1.0$  Myr while one in a typical halo has an orbital period of  $10 - 100$  Myr (if it is bound at all). Given that the clusters in our sample are all very young, we can easily conclude that the distribution of stars in the

halo (when present) must closely follow their original distribution at birth. Cores may have experienced some evolution (as we will see later) but it is also evident that their existence must be the result of the formation process. A consequence of this early evolutionary state is that strong halos are quite asymmetric and are not centered around their respective cores, as would be expected in very young clusters whose stars have not completed a single orbit around the center. We propose here that the existence of SOBAs and compact clusters can be traced to the existence of two broad types of cluster-forming Giant<sup>7</sup> Molecular Clouds (GMCs): “Super-GMCs”, characterized by very large masses and sizes of tens to a few hundred pc, and “Compact-GMCs”, smaller and maybe less massive but with higher central densities. A compact cluster with a strong halo would be the result of a “Compact-GMC-like” core inside a “Super-GMC”. The observed morphology of the nearby cloud OMC-1 (Wiseman & Ho 1998) strongly reminds of this type of arrangement: A compact core is surrounded by a series of linear structures or filaments which extend for tens of core radii (see Fig. 7). Of course, the progenitors of MYCs must be much larger than OMC-1 but more massive cores are also observed in other clouds (Evans 1999) and the hierarchical structure of OMC-1 suggests that the same type of structure could be present in larger GMCs. In this respect it is interesting to notice that “chains of stars” are readily visible in some of the SOBAs and massive halos of some of the youngest objects in our sample, such as 30 Doradus, NGC 604, NGC 2403-II, and NGC 4214-I-A, suggesting that they originated from molecular filaments.

It has been suggested that the most massive stars form by the coalescence of lower-mass stars (see Stahler et al. 2000 for a recent review). If that was the case, one should find that the fraction of very massive stars depends on the density of the cluster, since stellar collisions should be very rare in SOBAs but rather common in compact cores (Portegies Zwart et al. 1999). However, the analysis of a SOBA like NGC 604 reveals no obvious dearth of very massive stars. Hunter et al. (1996) analyzed the stellar photometry of the cluster and measured values for the IMF and the ratio of WR/O stars similar to those of R136. González Delgado & Pérez (2000) studied the integrated UV spectrum of NGC 604 and concluded that the best fit was provided by a 3 Myr old burst with a Salpeter IMF and  $M_{\text{up}} > 80 M_{\odot}$ , with the  $M_{\text{up}} \leq 60 M_{\odot}$  models clearly excluded. Therefore, either coalescence plays only a minor role in the formation of massive stars or the molecular filaments which appear to be the origin of SOBAs and halos contain compact subcores which are dense enough to cause a significant number of stellar collisions but not large enough to produce a compact cluster.

---

<sup>7</sup>Of course, “giant” should be understood in this context as implying a very large mass, not a very large size.

Another important consequence of the morphological dichotomy between compact clusters and SOBAs is the long-term survival of MYCs. Several processes contribute to the destruction of a cluster, of which the most important ones are two-body evaporation and tidal disruption by encounters with the galactic disk or by dynamical friction with the galactic halo (Fall 2001). Two-body evaporation dominates for very compact clusters while tidal processes control the fate of extended clusters, with both effects becoming more important for low-mass clusters. Tidal effects strongly depend on the galactic environment (a cluster close to a galactic nucleus is much more easily destroyed than one in a circular orbit in the outer halo) and the evolution of a cluster is controlled by stochastic events so it is not possible to give a precise mass-size survival range for a given age. However, an approximate rule is shown in Fig. 2 of Fall & Rees (1977) for the range of interest: A cluster with  $M \gtrsim 3 \cdot 10^4 M_{\odot}$  and  $r_{1/2}$  between 2 pc and 10 pc has a good chance of surviving after a Hubble time, while one outside this range is likely to be destroyed. Thus, SOBAs will likely disperse and compact clusters will likely lose their halos due to tidal effects. The fate of an object like R136 will depend on what fraction of its halo is able to retain. If it loses most of it, it could slip below the critical mass but if it retains the inner part it could survive for a Hubble time. In any case, SOBAs will not be able to continue existing for such a period of time and their components will mix with the rest of their parent galaxies. Therefore, a large fraction of MYCs are expected to disperse and at most 50% will be able to become the GCs of the future.

As it has been mentioned before, some of the cluster cores are double. There are two possible explanations for this: (1) A simple manifestation of the original structure of the molecular cloud, with two large mass concentrations instead of one collapsing simultaneously. (2) An initial collapse of one of the two concentrations followed by the induced collapse of the second one. The second process is called a *two-stage starburst* and is observed in the two most massive clusters in the LMC, 30 Doradus and N11 (Parker et al. 1992; Walborn et al. 1999). In a two-stage starburst there is an age difference of  $\approx 2 - 3$  Myr between the two stages and the final outcome can be a double cluster (N11) or a central core surrounded by a younger generation in its halo (30 Doradus). It would be interesting to obtain resolved spectroscopy of the clusters in the sample in order to decide whether double cores (or core-halo structures) are coeval or whether there is an age difference between them.

Finally we would like to discuss an aspect of the nomenclature which is affected by the previous discussion. In the last years, the term *Super Star Cluster* has become popular and it is applied to the progenitors of “old” globular clusters. In this paper we have avoided its use so far because, as we have seen, it was not clear whether all MYCs are expected to become GCs and, indeed, we have found that SOBAs are quite likely to disperse in a Hubble time. However, MYCs with compact cores are expected to survive for a Hubble time (even

though their halos may disperse) and it should be to those to which the term should be applied exclusively. We also recommend that a neutral term like MYC be applied to more distant unresolved objects with  $M_{V,\max} < -11$  or  $\gtrsim 3 \cdot 10^4 M_{\odot}$  until their structure can be analyzed.

### 3.2. The masses of NGC 1569-A and NGC 1705-I-A

Ho & Filippenko (1996) measured the velocity dispersions of NGC 1569-A and NGC 1705-I-A by cross-correlating their 5000–6280 Å spectra with a K5-M0 supergiant template. They obtained values of  $15.7 \pm 1.5 \text{ km s}^{-1}$  and  $11.4 \pm 1.5 \text{ km s}^{-1}$ , respectively, and then used the half-light radii measured by Meurer et al. (1995) to obtain masses of  $(3.3 \pm 0.5) \cdot 10^5 M_{\odot}$  and  $(8.2 \pm 2.1) \cdot 10^4 M_{\odot}$ , respectively. However, we point out that the FOC and PC images used by Meurer et al. (1995) to measure  $r_{1/2}$  were obtained previous to the first HST service mission and that in their data the core of NGC 1705-I-A was strongly saturated. NGC 1705-I-A may well be termed the “great saturator”, since most of the prop. ID 7506 WFPC2 images were also affected by this problem. However, as explained before, the saturation here was only minor and non-saturated data was available to correct for it. Furthermore, saturation affected only the central 9 pixels, where only  $\approx 35\%$  of the total corrected flux is contained, so the measurement of  $r_{1/2}$  after the extra flux addition in the central area should yield a correct value.

Our value for  $r_{1/2}$  for NGC 1569-A (2.1 pc) is in a reasonable agreement with those of Meurer et al. (1995) ( $1.7 \pm 0.2 \text{ pc}$ ) and O’Connell et al. (1994) ( $1.9 \text{ pc}$ )<sup>8</sup>. On the other hand, our value for  $r_{1/2}$  for NGC 1705-I-A (5.3 pc) is higher than the ones measured by those same authors ( $0.9 \pm 0.2 \text{ pc}$  and  $3.4 \text{ pc}$ , respectively), with the difference being especially significant in the first case. Given the pre-COSTAR character of their data and the strong saturation problems of the FOC images, we think that our values should be preferred.

The largest contribution to the uncertainty in the measured masses is the distance, which enters the calculation through  $r_{1/2}$ . Using the values for the uncertainties in the distance given by De Marchi et al. (1997) for NGC 1569 ( $\pm 0.6 \text{ Mpc}$ ) and by O’Connell et al. (1994) for NGC 1705 ( $\pm 2 \text{ Mpc}$ ), we arrive at values for the masses of NGC 1569-A and NGC 1705-I-A of  $(3.6 \pm 1.0) \cdot 10^5 M_{\odot}$  and  $(4.8 \pm 1.9) \cdot 10^5 M_{\odot}$ . These values clearly establish NGC 1569-A and NGC 1705-I-A as bona fide SSCs (i.e. globular cluster progenitors) and also solve an apparent contradiction in the Ho & Filippenko (1996) results: NGC 1569-A appeared to be

---

<sup>8</sup>We are converting all values to an assumed distance of 2.2 Mpc for NGC 1569 and 5.0 Mpc for NGC 1705.

$\approx 4$  times more massive than NGC 1705-I-A while at the same time having a similar  $M_V$  (and, since NGC 1705-I-A appears to be older than NGC 1569-A, the latter one is actually dimmer in  $M_{V,\text{max}}$ ). Now the results are consistent with both clusters having a similar mass-to-light ratio when reduced to the same age. However, one last word of caution should be spoken: since NGC 1569-A is now known to have a double core and the value derived here assumes spherical symmetry (Ho & Filippenko 1996), its mass may be slightly lower than what is published here, since some of the width of the line may be caused by the orbital motion of one core around the other and not by random stellar motions.

### 3.3. Early cluster evolution

We mentioned earlier that during most of the life of a cluster the two most important processes which determine its evolution are two-body evaporation and tidal disruption. In the first few million years, however, mass loss from stellar winds and SNe and binary heating are expected to play a dominant role in the case of SSCs. Even though the mass lost is a small fraction of the total mass ( $\approx 4\%$ ), this mass comes from deep inside the potential well and produces a significant expansion of the cluster (Portegies Zwart et al. 1999). The core is expected to expand by a factor of  $\approx 2$  in the first 7 Myr, with the exact value depending on the model and on the definition of radius chosen.

We decided to test this prediction with our data by checking whether there is a dependence of the average cluster radius with age. We included in our sample all the SSCs with a weak halo and those SSCs with a strong halo which showed a single non-elongated core (30 Doradus, NGC 2403-II, and NGC 4214-I-A). In order to establish a meaningful comparison, we used  $r_{1/4}$  for the weak-halo SSCs and we measured  $r_{1/8}$  for the strong-halo SSCs. Since all strong-halo SSCs have values of halo/(halo+core) luminosities  $\gtrsim 0.5$ ,  $r_{1/8}$  should be a good approximation (or at least a good upper bound) for the value of  $r_{1/4}$  in the absence of a halo. We discarded the strong-halo SSCs with a double or elongated core because we are interested in the evolution of the type of simple systems described by Portegies Zwart et al. (1999) with no external influences. The measured values of  $r_{1/8}$  for 30 Doradus, NGC 2403-II, and NGC 4214-I-A are 0.89 pc, 1.02 pc, and 1.05 pc, respectively. The results are plotted as a function of age in Fig. 8. The age errors are obtained from Table 3 while the errors in radius are estimated by assuming a measurement error of 1/4 of a pixel and a distance error of 20% (10% in the case of 30 Dor).

An apparent evolution is seen in Fig. 8. The average radius for the five clusters with most-likely age less than 7 Myr is 0.99 pc while that for the five clusters with most-likely age greater than 7 Myr is 1.71 pc. The effect may be somewhat stronger than what appears

in Fig. 8 if we consider that two of the points in the lower left part of the diagram could actually be below their represented positions: NGC 4214-I-A may be more compact if it is located closer than 4.1 Mpc (see previous note in section 2.3); also, R136 contains only  $\approx 10\%$  of the  $U$  flux of 30 Doradus, so  $r_{1/8}$  is clearly only an upper bound of what  $r_{1/4}$  would be in the absence of a halo. We can then conclude that the predicted expansion is apparently observed, though more clusters need to be measured and better data have to be obtained in order to confirm it. It is expected that a very young core like R136 will expand in the next few Myr until it reaches a size more similar to that of NGC 1705-I-A, which is also a typical size for a mature GC.

#### 4. SUMMARY

We have analyzed a sample of 27 nearby MYCs and we have confirmed the dichotomy between SSC cores and SSC halos/SOBAs. SSC cores are compact objects which have a good chance of lasting for a Hubble time, maybe retaining a part of their halos but losing most of them due to tidal interactions with their host galaxies. SOBAs are extended clusters which are expected to disperse rather quickly, thus producing a significant contribution to the field population of their host galaxies. This dichotomy places restrictions on the role of coalescence as the main mechanism for producing very massive stars and leads to some suggestions regarding the classification of massive clusters. We have found an interesting similarity between the morphologies of very young SOBAs and SSCs with strong halos on the one hand and that of the densest parts of galactic molecular clouds, suggesting that the first retain a memory of their previous stage. Our data have also enabled us to obtain new values for the masses of NGC 1569-A and NGC 1705-I-A and to verify the prediction that SSC cores should experience an expansion during their first few Myr of existence due to mass loss from stellar winds and SNe.

The author would like to thank Jennifer Wiseman, Georges Meylan, and an anonymous referee for helpful comments and/or discussion. Support for this work was provided by NASA through grant GO-8163.01-97A from the Space Telescope Science Institute, Inc., under NASA contract NAS5-26555.

#### REFERENCES

Arp, H., & Sandage, A. 1985, *AJ*, 90, 1163

- Barbá, R. H., et al. 2001, in preparation
- Buckalew, B. A., Dufour, R. J., Shopbell, P. L., & Walter, D. K. 2000, *AJ*, 120, 2402
- Calzetti, D., Meurer, G. R., Bohlin, R. C., Garnett, D. R., Kinney, A. L., Leitherer, C., & Storchi-Bergmann, T. 1997, *AJ*, 114, 1834
- Cerviño, M., Mas-Hesse, J. M., & Kunth, D. 2001, in preparation
- Da Costa, G. S. 2001, in *Extragalactic Star Clusters*, E. Grebel, D. Geisler, and D. Minniti (eds.), *Proc. IAU Symposium No. 207* (San Francisco: ASP), in press
- De Marchi, G., Clampin, M., Greggio, L., Leitherer, C., Nota, A., & Tosi, M. 1997, *ApJ*, 479, L27
- Drissen, L., Roy, J.-R., Moffat, A. F. J., & Shara, M. M. 1999, *AJ*, 117, 1249
- Drissen, L., Roy, J.-R., Robert, C., Devost, D., & Doyon, R. 2000, *AJ*, 119, 688
- Elson, R. A. W., & Fall, S. M. 1985, *ApJ*, 299, 211
- Evans, N. J., II. 1999, *Ann. Rev. Astron. Astrophys.*, 37, 311
- Fall, S. M. 2001, in *Extragalactic Star Clusters*, E. Grebel, D. Geisler, and D. Minniti (eds.), *Proc. IAU Symposium No. 207* (San Francisco: ASP), in press
- Fall, S. M., & Rees, M. J. 1977, *MNRAS*, 181, 37P
- Figer, D. F., Kim, S. S., Morris, M., Serabym, E., Rich, R. M., & McLean, I. S. 1999, *ApJ*, 525, 750
- Freeman, K. C., Illingworth, G., & Oemler, A. 1983, *ApJ*, 272, 488
- Gallagher, J. S., III, & Smith, L. S. 1999, *MNRAS*, 304, 540
- Gelatt, A. E., Hunter, D. A., & Gallagher, J. S., III. 2001, *PASP*, 113, 142
- González Delgado, R. M., Leitherer, C., Heckman, T., & Cerviño, M. 1997, *ApJ*, 483, 705
- González Delgado, R. M., & Pérez, E. 2000, *MNRAS*, 317, 64
- Ho, L. C., & Filippenko, A. V. 1996, *ApJ*, 472, 600
- Ho, L. C., & Filippenko, A. V. 2001, in preparation



- Holtzman, J., Burrows, C. J., Casertano, S., Hester, J. J., Trauger, J. T., Watson, A. M., & Worthey, G. 1995, *PASP*, 107, 1065
- Hunter, D. A. 1999, in *Wolf-Rayet Phenomena in Massive Stars and Starburst Galaxies*, K.A. van der Hucht, G. Koenigsberger and P. R. J. Eenens (eds.), *Proc. IAU Symposium No. 193* (San Francisco: ASP), 418
- Hunter, D. A., Baum, W. A., O’Neil, E. J., Jr., & Lynds, R. 1996, *ApJ*, 456, 174
- Hunter, D. A., O’Connell, R. W., Gallagher, J. S., III, & Smecker-Hane, T. A. 2000, *AJ*, 120, 2383
- Hunter, D. A., Shaya, E. J., Holtzman, J. A., Light, R. M., O’Neil, E. J., Jr., & Lynds, R. 1995, *ApJ*, 448, 179
- Hunter, D. A., & Thronson, H. A. 1995, *ApJ*, 452, 238
- Johnson, K. E., Leitherer, C., Vacca, W. D., & Conti, P. S. 2000, *AJ*, 120, 1273
- King, I. R. 1962, *AJ*, 67, 471
- Knödseder, J. 2000, *A&A*, 360, 539
- Larsen, S. S. 2001, in *Extragalactic Star Clusters*, E. Grebel, D. Geisler, and D. Minniti (eds.), *Proc. IAU Symposium No. 207* (San Francisco: ASP), in press
- Legrand, F., Kunth, D., Roy, J.-R., Mas-Hesse, J. M., & Walsh, J. R. 1997, *A&A*, 326, L17
- Leitherer, C., Goldader, J. F., González Delgado, R. M., Robert, C., Kune, D. F., de Mello, D. F., Devost, D., & Heckman, T. M. 1999, *ApJS*, 123, 3
- Leitherer, C., Vacca, W., Conti, P. S., Filippenko, A. V., Robert, C., & Sargent, W. L. W. 1996, *ApJ*, 465, 717
- Mackenty, J. W., Maíz-Apellániz, J., Pickens, C. E., Norman, C. A., & Walborn, N. R. 2000, *AJ*, 120, 3007
- Maíz-Apellániz, J. 2000, *PASP*, 112, 1138
- Maíz-Apellániz, J., et al. 2001, in preparation
- Maíz-Apellániz, J., & Cerviño, M. 2001, in preparation
- Maíz-Apellániz, J., & Walborn, N. R. 2001, in *Galaxies and their constituents at the Highest Angular Resolution*, *Proc. IAU Symposium No. 205* (San Francisco: ASP), in press

- Malamuth, E. M., Waller, W. H., & Parker, J. W. 1996, *AJ*, 111, 1128
- Mas-Hesse, J. M., & Kunth, D. 1999, *A&A*, 349, 765
- Massey, P., & Hunter, D. A. 1998, *ApJ*, 493, 180
- Melnick, J., Moles, M., & Terlevich, R. 1985, *A&A*, 149, L24
- Meurer, G. R., Heckman, T. M., Leitherer, C., Kinney, A., Robert, C., & Garnett, D. R. 1995, *AJ*, 110, 2665
- Moffat, A. F. J., Drissen, L., & Shara, M. M. 1994, *ApJ*, 436, 183
- O’Connell, R. W., Gallagher, J. S., III, & Hunter, D. A. 1994, *ApJ*, 433, 65
- Parker, J. W., Garmany, C. D., Massey, P., & Walborn, N. R. 1992, *AJ*, 103, 1205
- Portegies Zwart, S. F., Makino, J., McMillan, S. L. W., & Hut, P. 1999, *A&A*, 348, 117
- Stahler, S. W., Palla, F., & Ho, P. T. P. 2000, in *Protostars and Planets IV*, 121
- Walborn, N. R., Barbá, R. H., Brandner, W., Rubio, M., Grebel, E. K., & Probst, R. G. 1999, *AJ*, 117, 225
- Walborn, N. R., & Blades, J. C. 1997, *ApJS*, 112, 457
- Walborn, N. R., Maíz-Apellániz, J., & Barbá, R. H. 2001, in preparation
- Weigert, G., & Baier, G. 1985, *A&A*, 150, L18
- Whitmore, B. C., Zhang, Q., Leitherer, C., Fall, S. M., Schweizer, F., & Miller, B. W. 1999, *AJ*, 118, 1551
- Wiseman, J. J., & Ho, P. T. P. 1998, *ApJ*, 502, 676
- Zhang, Q., & Fall, S. M. 1999, *ApJ*, 527, L81

Table 1. Archival HST/WFPC2 data used for this work. The main filter is the one used to measure the radial profile. The last column indicates whether the cluster was observed using the PC or one of the WF chips.

Galaxy	Clusters	Main filter	V filter	Proposal ID(s)	PC/WF
LMC	30 Dor	F336W	F555W	5589,5114,8163	PC+WF
M33	NGC 595	F336W	F547M	5384	PC
	NGC 604	F336W	F555W	5237	WF
I Zw 18	I,II	F336W	F555W	5309	PC
NGC 1569	A,B,C	F336W	F555W	6423	PC
NGC 1705	I-A,I-B	F380W	—	7506	PC
NGC 2403	I-A,I-B,I-C,II	F439W	F547M	5383	PC
	IV	F439W	F547M	5383	WF
NGC 4214	I-A,I-B	F336W	F555W	6716	PC
	I-D,II-C,V,VI,VII	F336W	F555W	6569	WF
NGC 4449	N-1,N-2	F336W	F547M	6716	PC
NGC 5253	I,IV,VI	F336W	F547M	6716,6524	PC

Table 2. Input data. Extinctions and ages are calculated from a combination of literature data and integrated colors. The fourth column indicates the method used to determine the age.

Cluster	$E(B - V)$	Age Myr	Method	$d$ Mpc	References
30 Dor	0.35	$2.0 \pm 1.0$	CMD,UVS,OSF	0.05	1,2,3
NGC 595	0.33	$4.0 \pm 1.0$	CMD,UVS,OSF	0.84	4,5
NGC 604	0.20	$3.5 \pm 0.5$	CMD,UVS,OSF,Neb	0.84	6,7
I Zw 18-I	0.05	$3.5 \pm 0.5$	CMD,OSF,Neb	10.00	8,9
I Zw 18-II	0.20	$3.0 \pm 2.0$	Neb,IC	10.00	8
NGC 1569-A	0.55	$6.0 \pm 4.0$	OS,IC	2.20	10,11
NGC 1569-B	0.55	$11.0 \pm 3.0$	OS,IC	2.20	10,11
NGC 1569-C	1.00	$3.0 \pm 2.0$	OSF,Neb,IC	2.20	12,13
NGC 1705-I-A	0.06	$15.0 \pm 5.0$	OSF,IC	5.00	14,15
NGC 1705-I-B	0.06	$10.0 \pm 8.0$	IC	5.00	14,15
NGC 2403-I-A	0.28	$6.0 \pm 4.0$	OSF,IC	3.20	16
NGC 2403-I-B	0.28	$6.0 \pm 4.0$	OSF,IC	3.20	16
NGC 2403-I-C	0.28	$6.0 \pm 4.0$	OSF,IC	3.20	16
NGC 2403-II	0.28	$4.5 \pm 2.5$	OSF,IC	3.20	16
NGC 2403-IV	0.28	$4.5 \pm 2.5$	OSF,IC	3.20	16
NGC 4214-I-A	0.03	$3.5 \pm 0.5$	UVS,OSF,Neb,IC	4.10	6,17,18
NGC 4214-I-B	0.35	$3.5 \pm 0.5$	OSF,Neb,IC	4.10	6,17
NGC 4214-I-D	0.02	$9.0 \pm 3.0$	OSF,Neb,IC	4.10	6,17
NGC 4214-II-C	0.20	$2.0 \pm 1.0$	OSF,Neb	4.10	6,17
NGC 4214-V	0.03	$11.0 \pm 5.0$	IC	4.10	17
NGC 4214-VI	0.05	$11.0 \pm 5.0$	IC	4.10	17
NGC 4214-VII	0.03	$11.0 \pm 5.0$	OSF,IC	4.10	17
NGC 4449-N-1	0.25	$11.0 \pm 5.0$	IC	3.90	19
NGC 4449-N-2	0.25	$3.0 \pm 2.0$	IC	3.90	19
NGC 5253-I	0.05	$11.5 \pm 2.5$	IC	4.10	20
NGC 5253-IV	0.05	$3.5 \pm 0.5$	OSF,Neb,IC	4.10	20
NGC 5253-VI	0.05	$11.0 \pm 3.0$	IC	4.10	20

Age methods CMD: Color-magnitude diagram, UVS: Ultraviolet spectroscopy, OSF: Optical spectral features (WR, Ca triplet), Neb: Nebular equivalent widths and/or structure, IC: Integrated colors.

References 1: Walborn & Blades (1997); 2: Massey & Hunter (1998); 3: Barbá et al. (2001); 4: Malamuth et al. (1996); 5: Mas-Hesse & Kunth (1999); 6: Maíz-Apellániz (2000); 7: González Delgado & Pérez (2000); 8: Hunter & Thronson (1995); 9: Legrand et al. (1997); 10: De Marchi et al. (1997); 11: González Delgado et al. (1997); 12: Hunter et al. (2000); 13: Buckalew et al. (2000); 14: O’Connell et al. (1994); 15: Ho & Filippenko (1996); 16: Drissen et al. (1999); 17: Mackenty et al. (2000); 18: Leitherer et al. (1996); 19: Gelatt et al. (2001); 20: Calzetti et al. (1997).

Table 3. Results.  $r_{1/4}$ ,  $r_{1/2}$ , and  $r_{3/4}$  are obtained from the measured angular sizes and the distances. Age-corrected absolute  $V$  magnitudes are calculated from the measured apparent  $V$  magnitudes and the data in Table 2. Two values of  $M_{V,\max}$  are given, one for the whole cluster and another one for the area within 3 pc of the center.

Cluster	$r_{1/4}$ pc	$r_{1/2}$ pc	$r_{3/4}$ pc	$m_V$	$M_{V,\max}$ tot	$M_{V,\max}$ < 3 pc	Notes
30 Dor	3.3	9.2	15.5	8.0	-12.4	-10.7	C,St
NGC 595	14.4	26.9	38.0	14.3	-11.4	-8.5	SOBA
NGC 604	18.4	28.4	44.3	12.7	-12.6	-8.3	SOBA
I Zw 18-I	29.1	46.3	75.0	17.0	-13.2	-6.3	SOBA
I Zw 18-II	27.8	50.4	68.9	18.4	-12.3	-6.8	SOBA
NGC 1569-A	0.9	2.1	5.3	14.6	-14.1	-13.5	C,Wk,Db
NGC 1569-B	1.4	3.7	9.5	15.4	-14.1	-13.2	C,Wk
NGC 1569-C	1.0	2.9	4.2	17.1	-12.8	-11.8	C,Wk,Db
NGC 1705-I-A	1.5	5.3	20.5	14.7	-15.4	-14.5	C,Wk,Nb
NGC 1705-I-B	1.9	2.7	4.9	18.1	-11.6	-11.2	C,Wk,Nb
NGC 2403-I-A	11.0	20.6	31.1	16.0	-12.6	-9.6	SOBA
NGC 2403-I-B	14.8	26.3	33.1	16.7	-12.0	-8.6	SOBA
NGC 2403-I-C	9.9	19.6	33.4	17.6	-11.0	-7.4	SOBA
NGC 2403-II	2.0	11.8	27.2	15.1	-13.4	-11.9	C,St
NGC 2403-IV	9.3	30.0	46.7	15.7	-12.7	-10.4	C,St,Db
NGC 4214-I-A	2.1	16.5	38.9	14.5	-13.7	-11.9	C,St
NGC 4214-I-B	21.5	33.0	51.8	15.6	-13.6	-9.5	SOBA
NGC 4214-I-D	9.9	15.3	27.6	17.2	-12.3	-9.2	SOBA
NGC 4214-II-C	16.6	21.7	29.2	18.1	-11.4	-8.4	SOBA
NGC 4214-V	52.5	83.9	127.1	16.0	-13.3	-8.2	SOBA
NGC 4214-VI	20.9	35.9	58.5	18.1	-11.3	-7.4	SOBA
NGC 4214-VII	24.8	40.4	56.9	17.0	-12.3	-7.7	SOBA
NGC 4449-N-1	6.9	16.9	29.3	14.5	-15.4	-13.0	C,St,Nb,El
NGC 4449-N-2	2.2	5.8	10.6	16.4	-12.4	-10.9	C,St,Nb,El
NGC 5253-I	2.0	4.0	7.5	16.9	-12.4	-11.9	C,Wk
NGC 5253-IV	6.2	13.8	19.4	16.3	-11.9	-10.4	C,St,Db
NGC 5253-VI	1.7	3.1	6.1	18.0	-11.3	-11.1	C,Wk

Notes C: Compact cluster, SOBA: Scaled OB Association.  
Wk,St: Weak (<40%), Strong (>40%) halo/total ratio.  
Db: Double core ( $\lesssim 7$  pc separation), Nb: Nearby ( $\lesssim 30$  pc) cluster present.  
El: Elongated core.

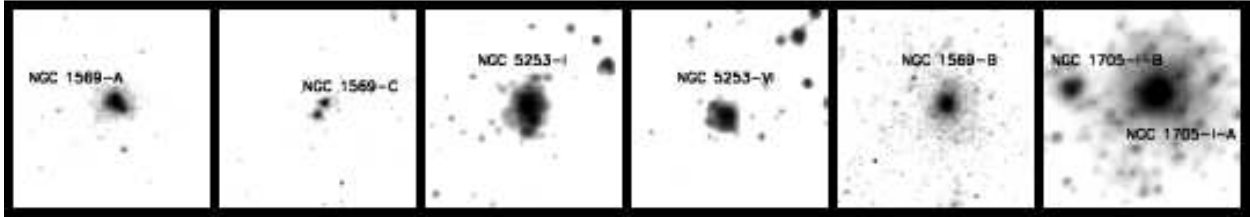


Fig. 1.— F380W (NGC 1705 field) or F336W (rest) WFPC2/HST images of the compact clusters in the sample with weak halos. The images have been resampled in order to use the same linear scale in all cases, with the field sizes being  $50 \text{ pc} \times 50 \text{ pc}$ . The orientation in each case is that of the original archival image.

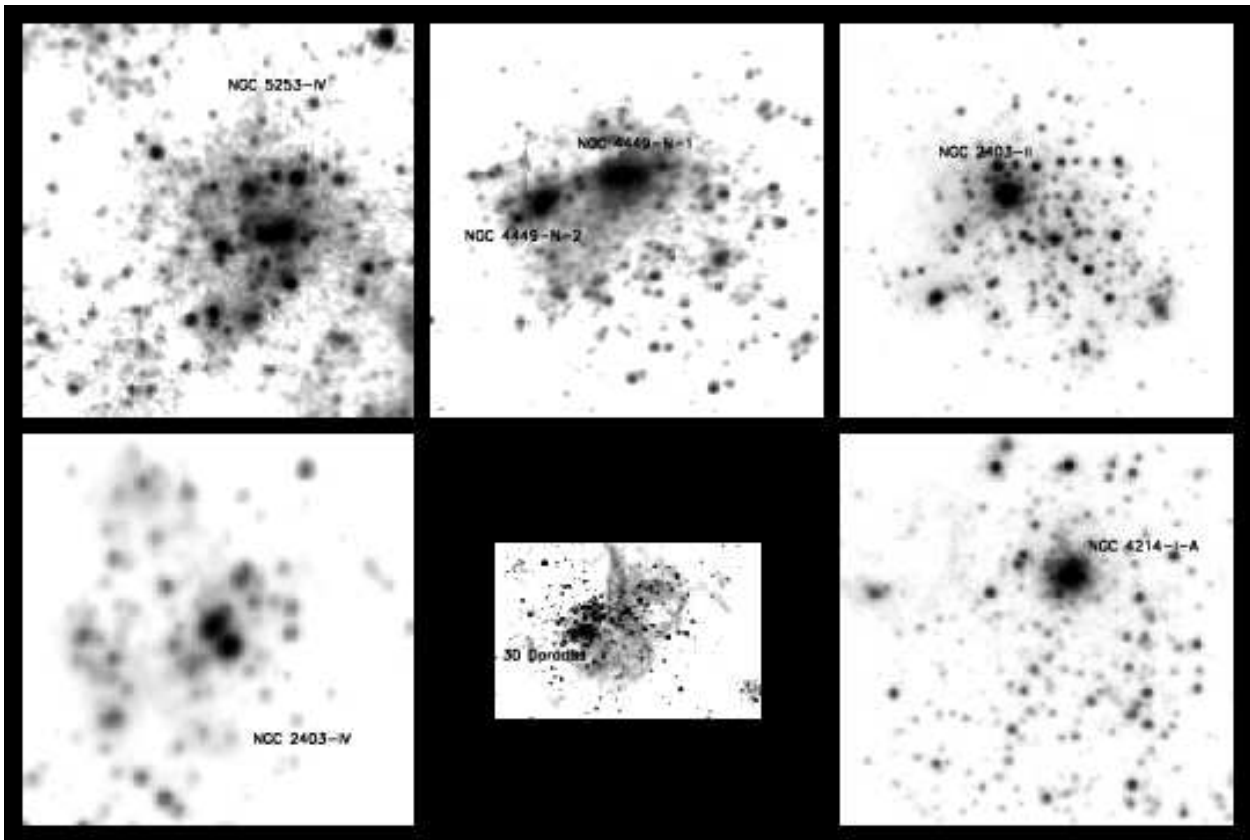


Fig. 2.— Same as Fig. 1 for the compact clusters in the sample with strong halos. The NGC 2403 fields were obtained with the F439W filter. The linear scale is the same and the field sizes are  $100 \text{ pc} \times 100 \text{ pc}$ , except for the 30 Doradus field, which is  $68 \text{ pc} \times 45 \text{ pc}$ .

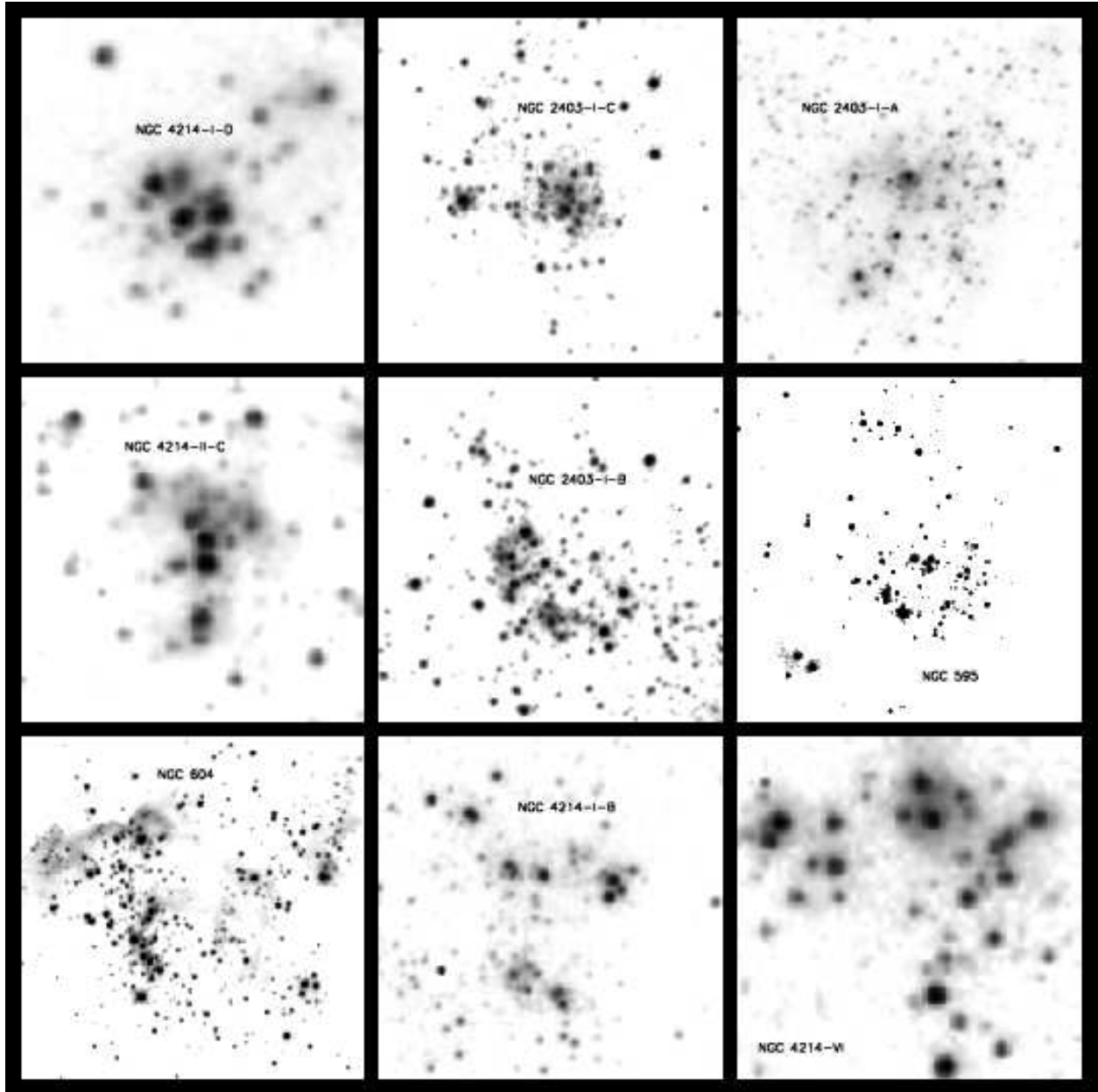


Fig. 3.— (a) Same as Fig. 2 for the SOBAs the sample. The field sizes are  $100 \text{ pc} \times 100 \text{ pc}$ .

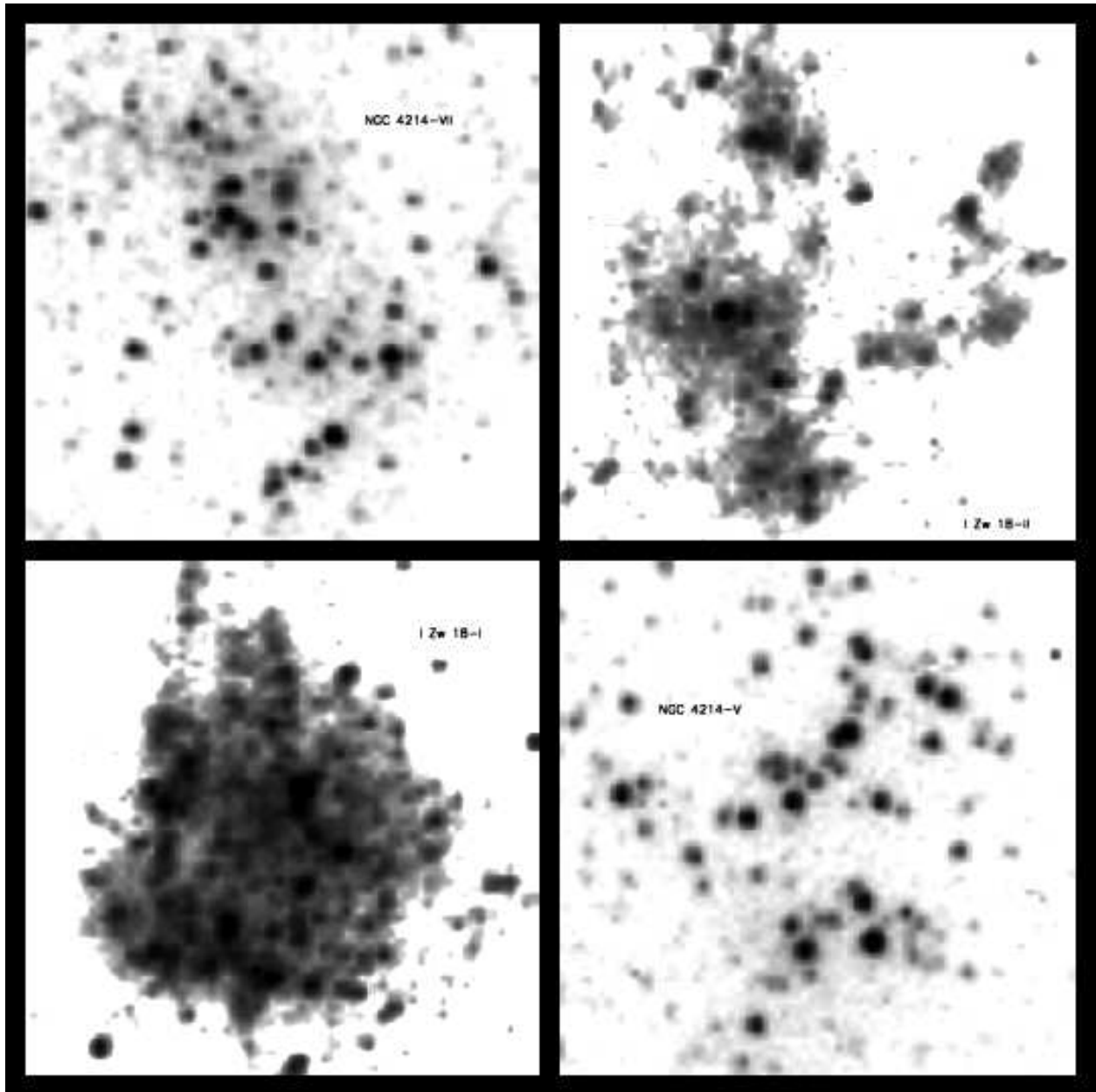


Fig. 3.— (b) Continued. The field sizes are  $150 \text{ pc} \times 150 \text{ pc}$ .



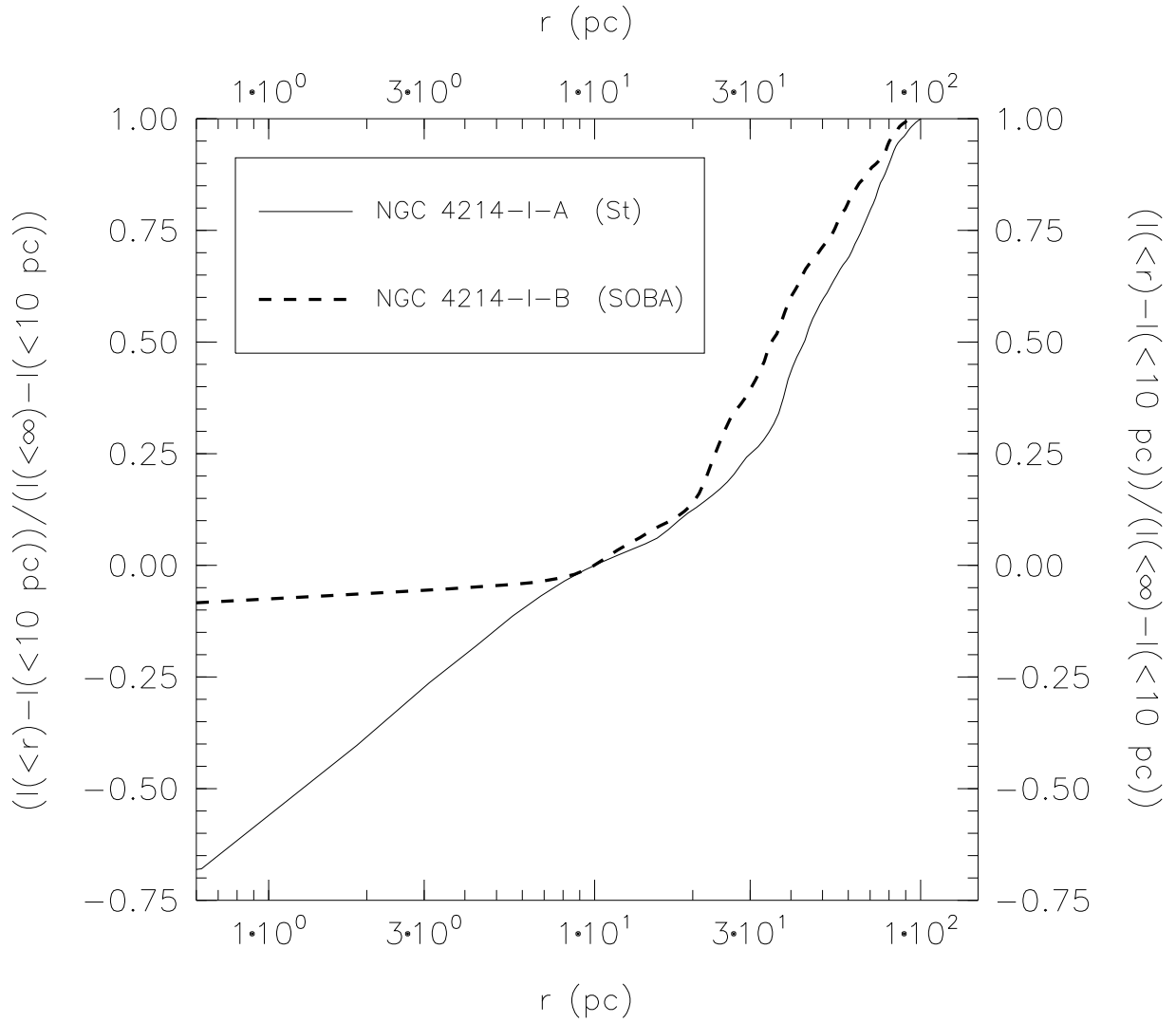


Fig. 4.— Intensity profiles for a compact cluster with a strong halo and for a SOBA. Note the similarity for  $r > 10$  pc.

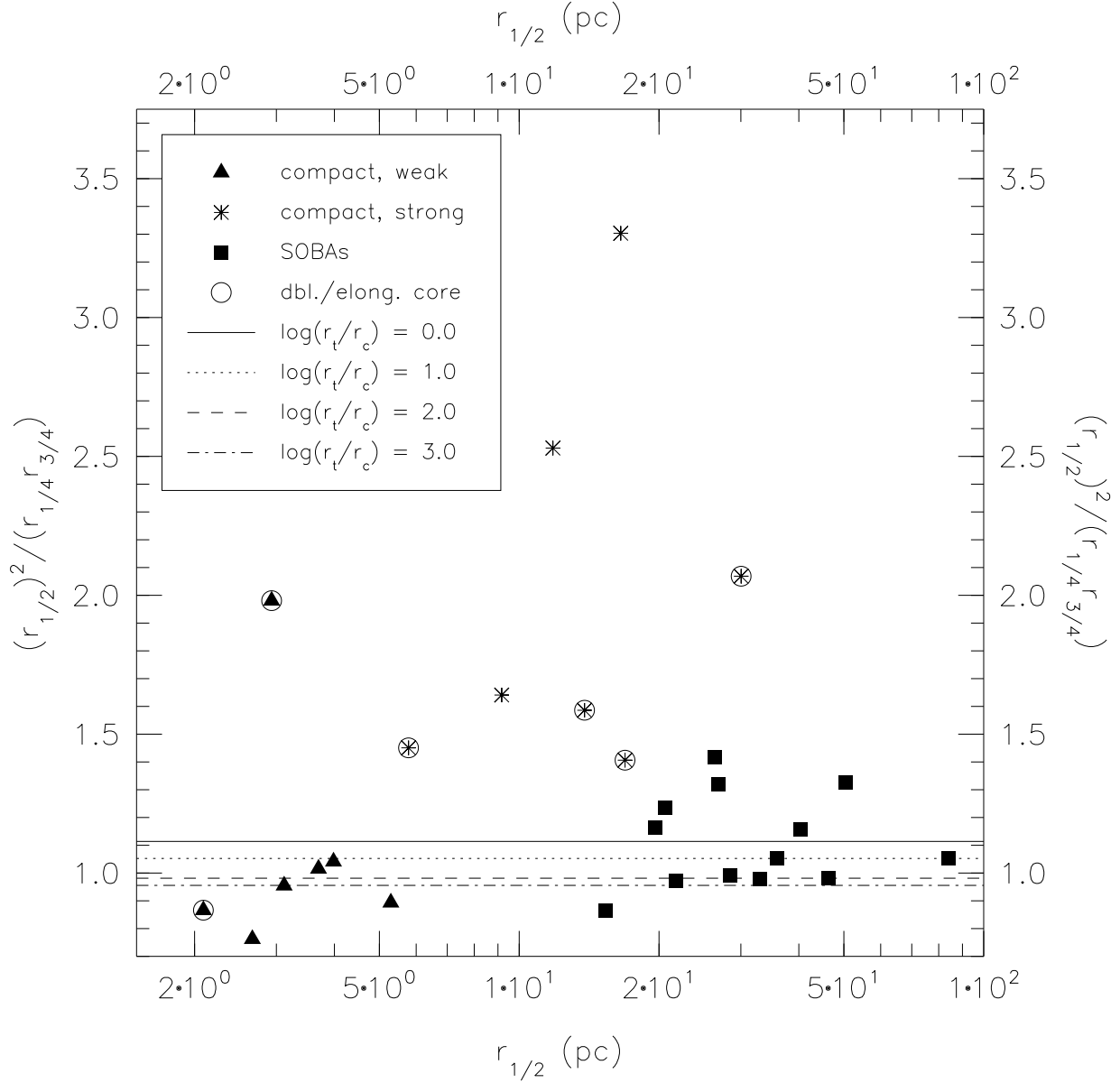


Fig. 5.—  $\alpha \equiv r_{1/2}^2 / (r_{1/4} r_{3/4})$  as a function of  $r_{1/2}$  plot which shows the different regions occupied by compact clusters with a weak halo, compact clusters with a strong halo, and SOBAs. Compact clusters with a double or elongated core are marked with a circle around their symbol. The horizontal lines indicate the expected values for different King models.

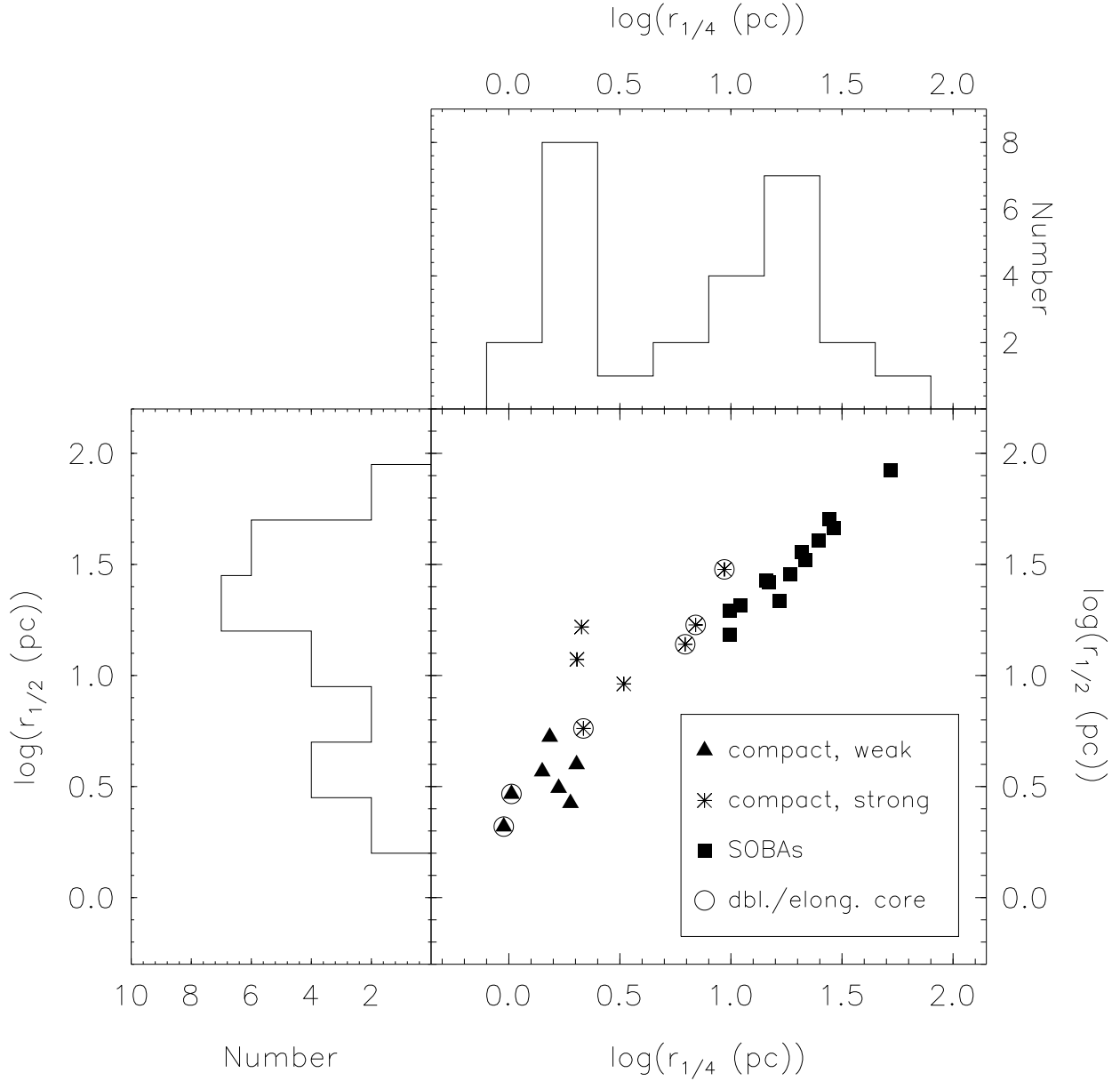


Fig. 6.— Half-light radius vs. quarter-light radius plot for the 27 clusters in the sample. Compact clusters with a double or elongated core are marked with a circle around their symbol. The top and left plots are the histograms for each axis.

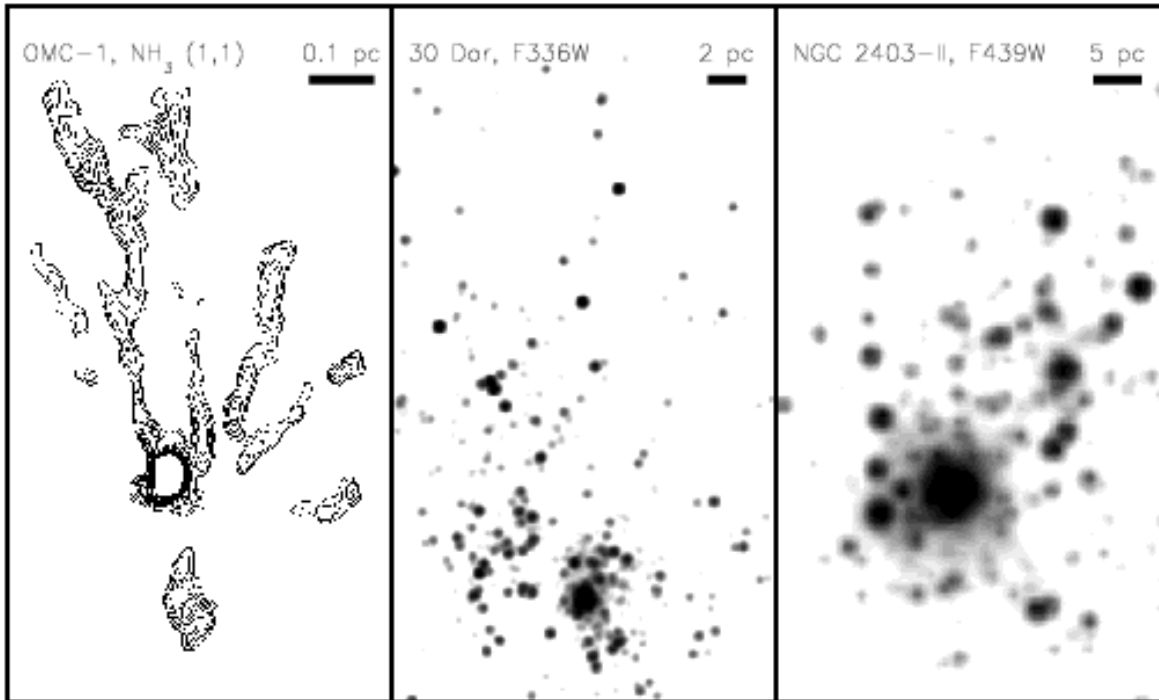


Fig. 7.— A comparison between the structures observed in the dense material of a galactic star-forming molecular cloud (OMC-1, adapted from Wiseman & Ho 1998) and in two of the compact clusters with strong halos in our sample. Even though the scales are quite different, in both cases the same core + quasiradial filamentary structure is observed. Since structures in molecular clouds are apparently hierarchical, it appears likely that the “chains of stars” in the cluster halos are a consequence of the original mass distribution of the parent cloud.

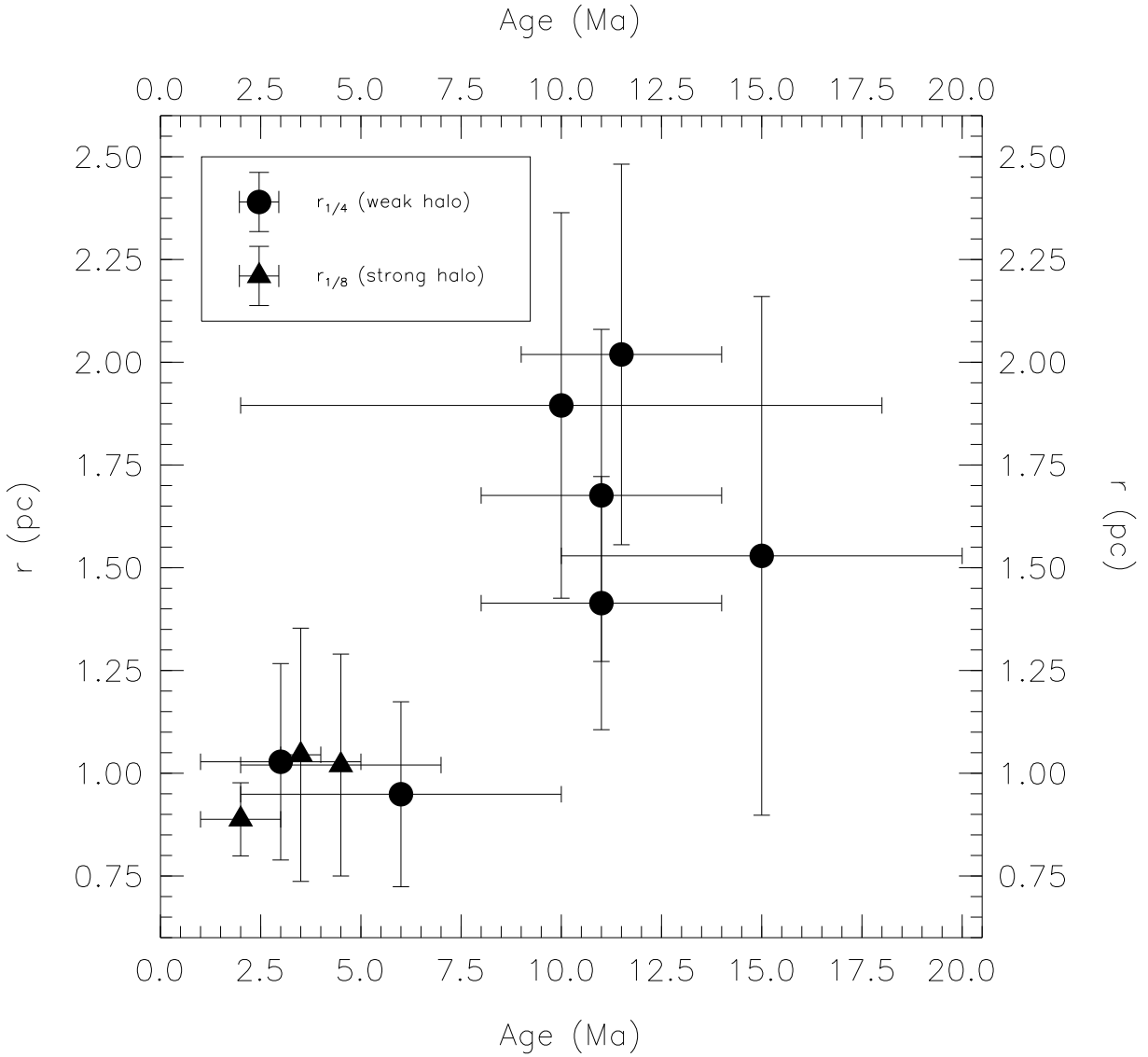


Fig. 8.— Radius as a function of age for the compact clusters in the sample. For objects with weak halos,  $r_{1/4}$  is the plotted radius, while for objects with strong halos it is  $r_{1/8}$ . For clusters with strong halos only the cases in which the core is not double or elongated are shown.